

SUPPLEMENTARY MATERIAL

GABA promotes the competitive selection of dendritic spines by
controlling local dendritic Ca²⁺ signaling

Tatsuya Hayama^{1,4}, Jun Noguchi^{1,4}, Satoshi Watanabe^{1,4}, Noriko Takahashi^{1,4},
Akiko Hayashi-Takagi^{1,4,5}, Graham C.R. Ellis-Davies², Masanori Matsuzaki³⁻⁵, &
Haruo Kasai^{1,4}

¹Laboratory of Structural Physiology, Center for Disease Biology and Integrative
Medicine, Faculty of Medicine, University of Tokyo, Bunkyo-ku, Tokyo 113-0033

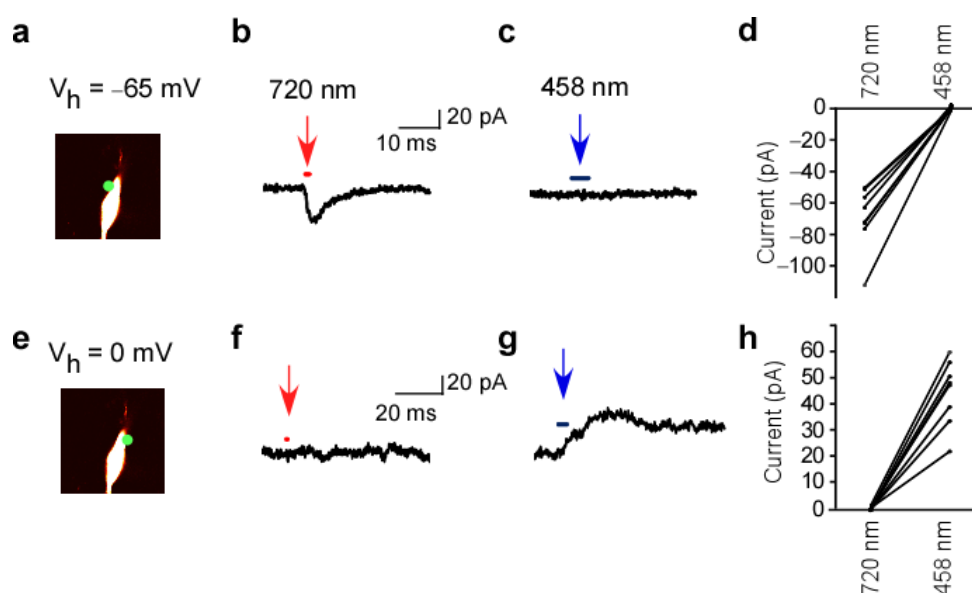
²Department of Neuroscience, Mount Sinai School of Medicine, New York, NY
10029, USA

³Division of Brain Circuits, National Institute for Basic Biology, The Graduate
University of Advanced Studies (Sokendai), Okazaki 444-8585, Japan

⁴CREST, Japan Science and Technology Agency, 4-1-8 Honcho, Kawaguchi,
Saitama 332-0012, Japan

⁵PRESTO, Japan Science and Technology Agency, 4-1-8 Honcho, Kawaguchi,
Saitama 332-0012, Japan

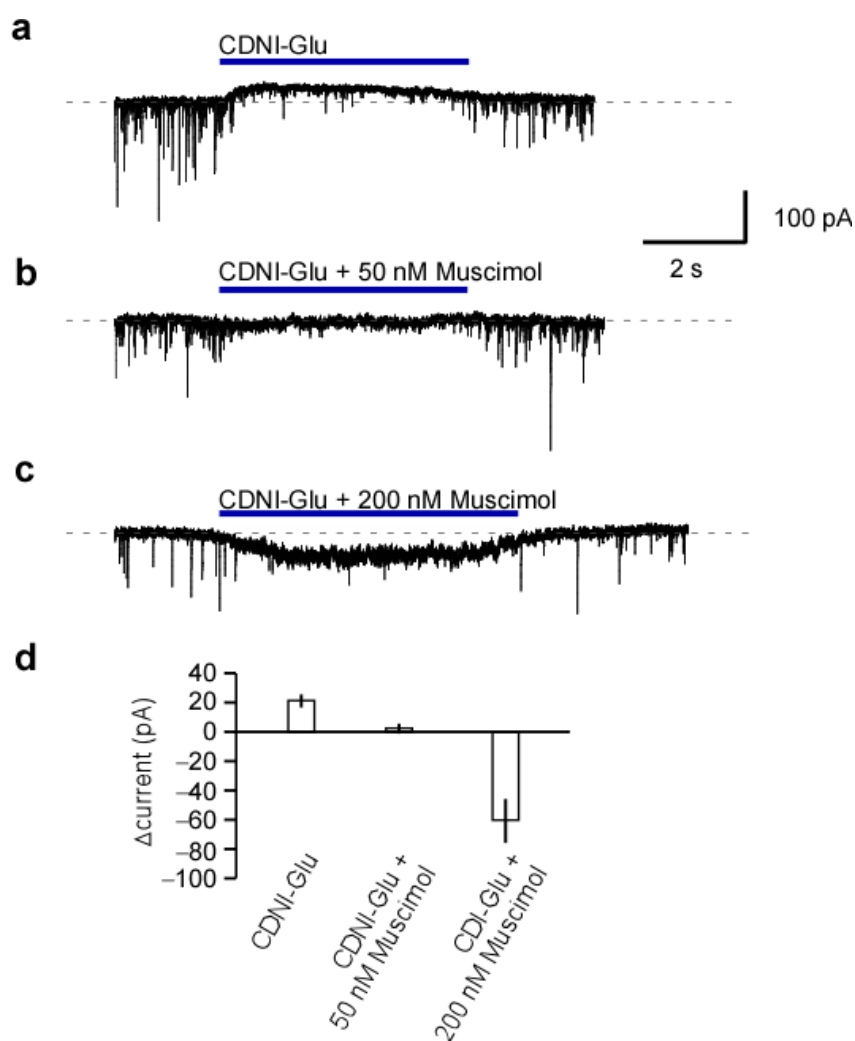
Supplementary Figure 1



Selectivity of two-color uncaging of glutamate and gamma-aminobutyric acid (GABA) in the presence of both CDNI-glutamate (2 mM) and RuBi-GABA (0.05 mM)

(a, e) The soma of the neuron where two-color uncaging was applied to the green spots. (b, c) Activation of a rapid inward current occurred at the holding membrane potential of -65 mV with the mode-locked laser at 720 nm (6 mW, 0.6 ms) in **b** but not with the blue laser (0.2 mW, 4 ms) in **c** on the same spot shown in **a**. (f, g) Activation of a slow outward current did not occur with the mode-locked laser in **f** but with the blue laser in **g** on the spot in **e** at the holding membrane potential of 0 mV. (d, h) Comparisons of the amplitudes of currents evoked either by a mode-locked laser at 720 nm or continuous laser at 458 nm on the same positions at the holding membrane potential of -65 mV in **d** and of 0 mV in **h**. CDNI-glutamate, 4-carboxymethoxy-5,7-dinitroindoliny-glutamate; RuBi-GABA, ruthenium-based GABA.

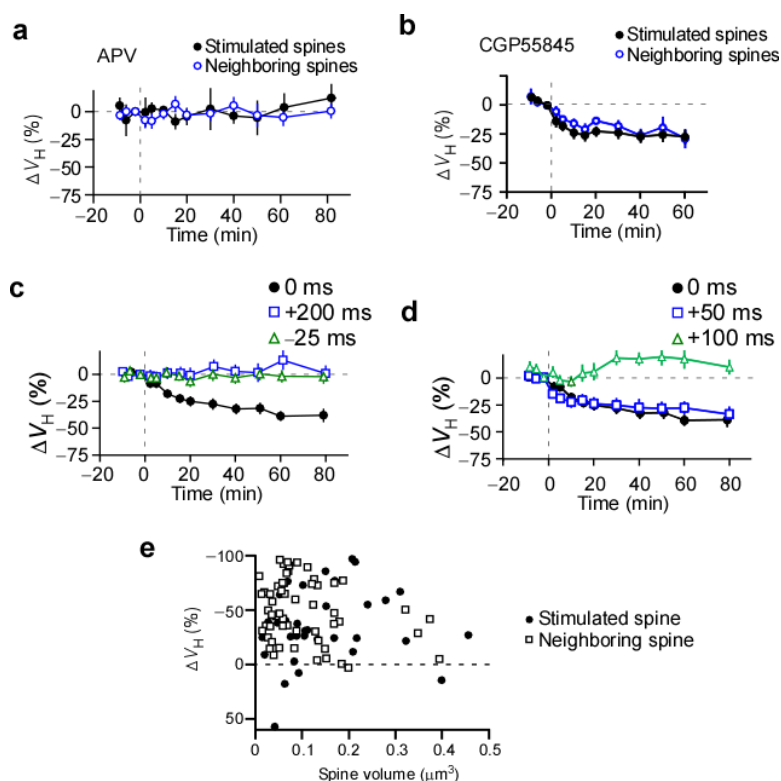
Supplementary Figure 2



Actions of CDNI-glutamate and muscimol on tonic GABA-mediated currents

Currents recorded with whole-cell voltage clamping were obtained with the CsCl-containing intracellular solution in the presence of CNQX (10 μ M), APV (50 μ M), and tetrodotoxin (1 μ M). **(a)** Inhibition of miniature inhibitory postsynaptic currents (IPSCs) and tonic inward currents evoked by the puffing of CDNI-glutamate. **(b)** Restoration of the tonic currents with the added presence of 50 nM muscimol. **(c)** Mediation of an inward current with an amplitude similar to that of miniature IPSCs by 200 nM muscimol in the presence of CDNI-glutamate. **(d)** Mean amplitudes of CDNI-glutamate induced currents obtained from 3–6 cells, 3–6 slices, 3–5 rats.

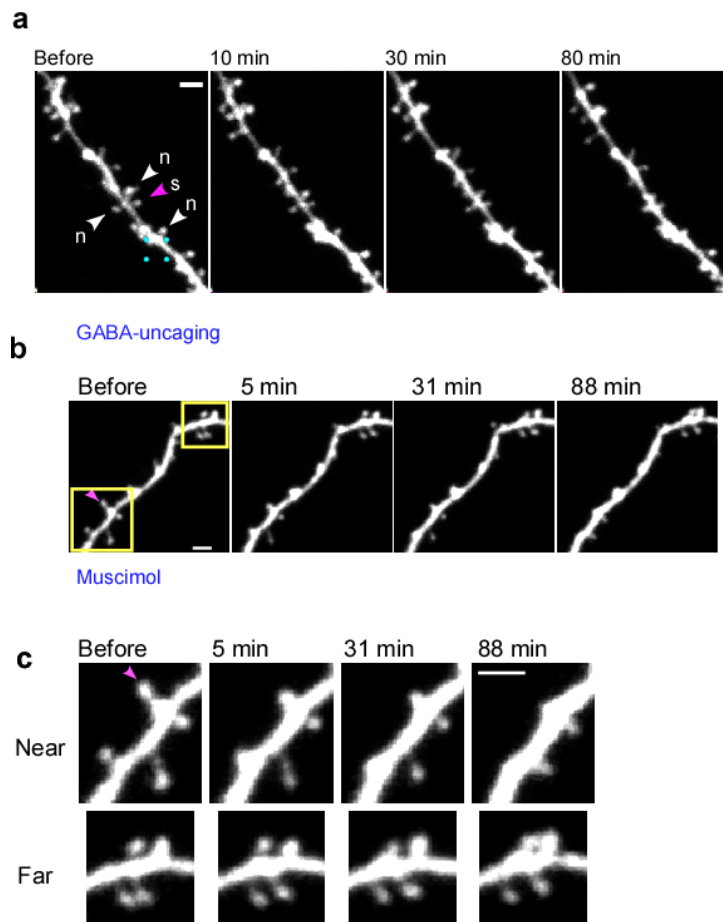
Supplementary Figure 3



Time courses of spine shrinkage that were induced by the spike-timing protocol with GABA uncaging at the dendritic shaft

(a) Averaged time courses of the volumes of stimulated (4 spines, 4 dendrites, 4 slices, 2 rats) and neighboring spines (9 spines, 4 dendrites, 4 slices, 2 rats) in the presence of APV. (b) Averaged time courses of the volumes of stimulated (5 spines, 5 dendrites, 4 slices, 3 rats) and neighboring spines (17 spines, 5 dendrites, 4 slices, 3 rats) in the presence of CGP55845. (c, d) Time courses of the changes in spine volumes when GABA uncaging was affected at spike onset (0 ms, 33 spines, 14 dendrites, 14 slices, 10 rats), 50 ms (+50 ms, 19 spines, 4 dendrites, 4 slices, 3 rats), 100 ms (+100 ms, 14 spines, 4 dendrites, 4 slices, 3 rats), and 200 ms preceding the spike (+200 ms, 19 spines, 6 dendrites, 6 slices, 4 rats) or 25 ms after the spike (−25 ms, 16 spines, 5 dendrites, 5 slices, 3 rats). The data are presented as mean \pm s.e.m. (e) Correlations between the initial volumes of spines and changes in spine volumes, which were obtained from the experiments with GABA uncaging or muscimol. The correlation coefficients are -0.13 and 0.25 for stimulated and neighboring spines, respectively, and the P values are 0.48 and 0.054 (34–56 spines), respectively.

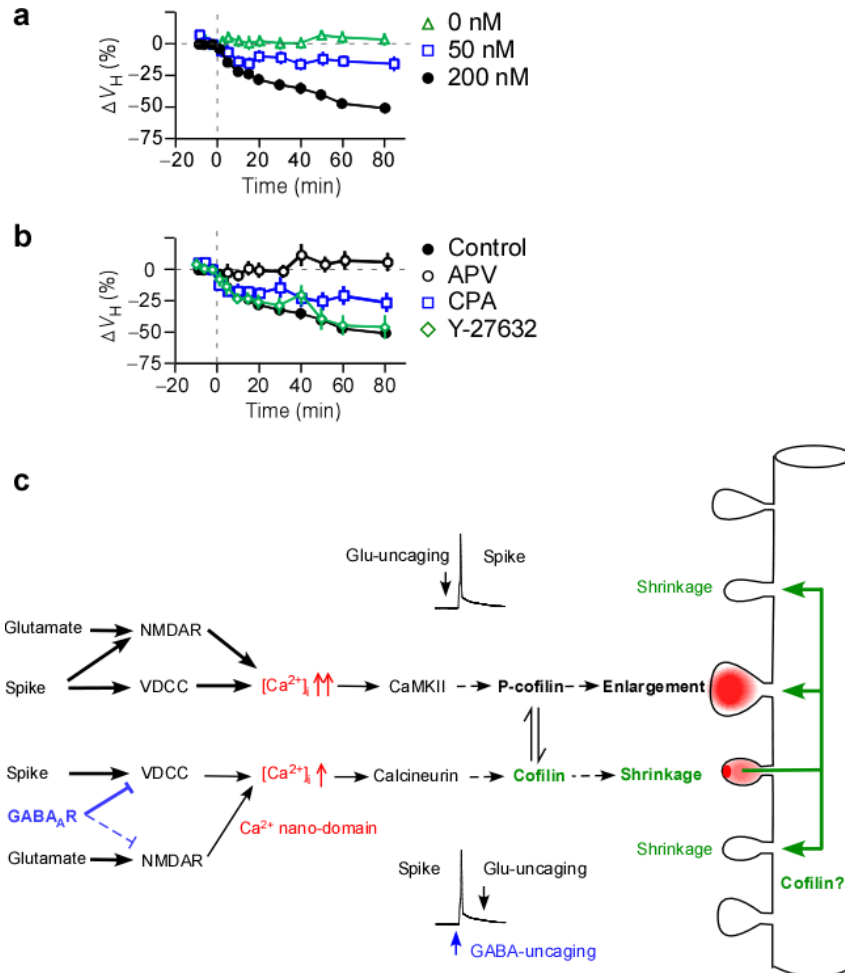
Supplementary Figure 4



Confinement of spine shrinkage within 15 μm from the spine subjected to the LTD protocol

(a) A large-scale image of dendrites where spine shrinkage was induced with glutamate uncaging at a single spine (“s,” magenta arrow head) and with GABA uncaging at the dendritic shaft (blue points). The neighboring spines that displayed shrinkage are denoted by “n.” The soma was located at the right side of the dendrite. (b) A large-scale image of dendrites whose lower and upper corners are presented in c, and where spine shrinkage was induced in the presence of 200 nM muscimol. Spine shrinkage was confined within 15 μm . Scale bar, 2 μm . A red arrow indicates a stimulated spine. The soma was located at the left of the dendrite. (c) Magnified images of the near and far regions in b of the dendrite relative to the site where the LTD protocol was applied.

Supplementary Figure 5

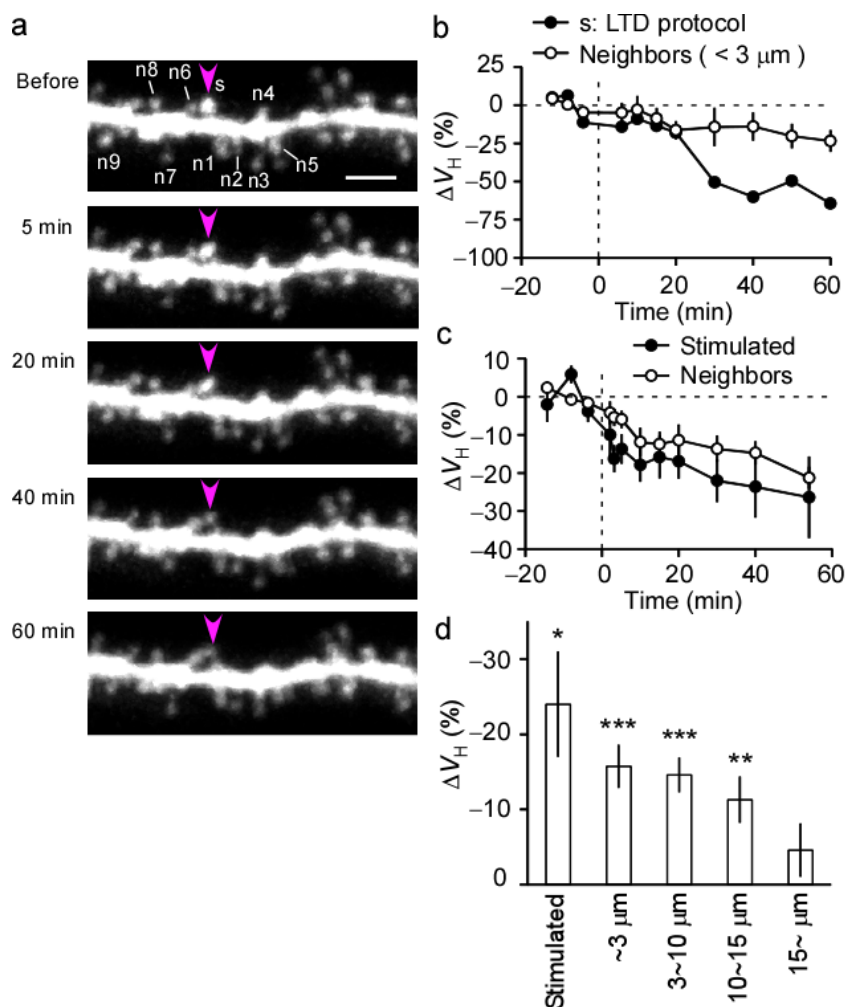


Signaling mechanisms for spine shrinkage

(a) Time courses of spine shrinkage in the presence of 0 nM (24 spines, 15 dendrites, 8 slices, 5 rats), 50 nM (28 spines, 11 dendrites, 7 slices, 4 rats), or 200 nM muscimol (56 spines, 18 dendrites, 17 slices, 14 rats). (b) Time courses of spine shrinkage in the further presence of APV (50 μ M, 41 spines, 13 dendrites, 6 slices, 4 rats), cyclopiazonic acid (CPA; 30 μ M, 23 spines, 8 dendrites, 4 slices, 2 rats), or Y-27632 (10 μ M, 21 spines, 8 dendrites, 3 slices, 3 rats). (c) The LTD protocol in the presence of GABAergic inhibition induces moderate increases in cytosolic Ca^{2+} concentrations ($[Ca^{2+}]_i$) and the

Ca^{2+} nanodomain of N-methyl-D-aspartate (NMDA) receptors, both of which are sensed by calcineurin. This results in the dephosphorylation and activation of the actin-depolymerizing factor (ADF)/cofilin. Active cofilin may diffuse along a dendrite up to 15 μm and induce the shrinkage of stimulated and surrounding spines. Conversely, the stimulation of NMDA receptors with the LTP protocol gives rise to large increases in the $[\text{Ca}^{2+}]_i$ that is sufficient to activate Ca^{2+} /calmodulin protein kinase II and phosphorylate (P)-cofilin for spine enlargement, which can outcompete the dephosphorylation of cofilin.

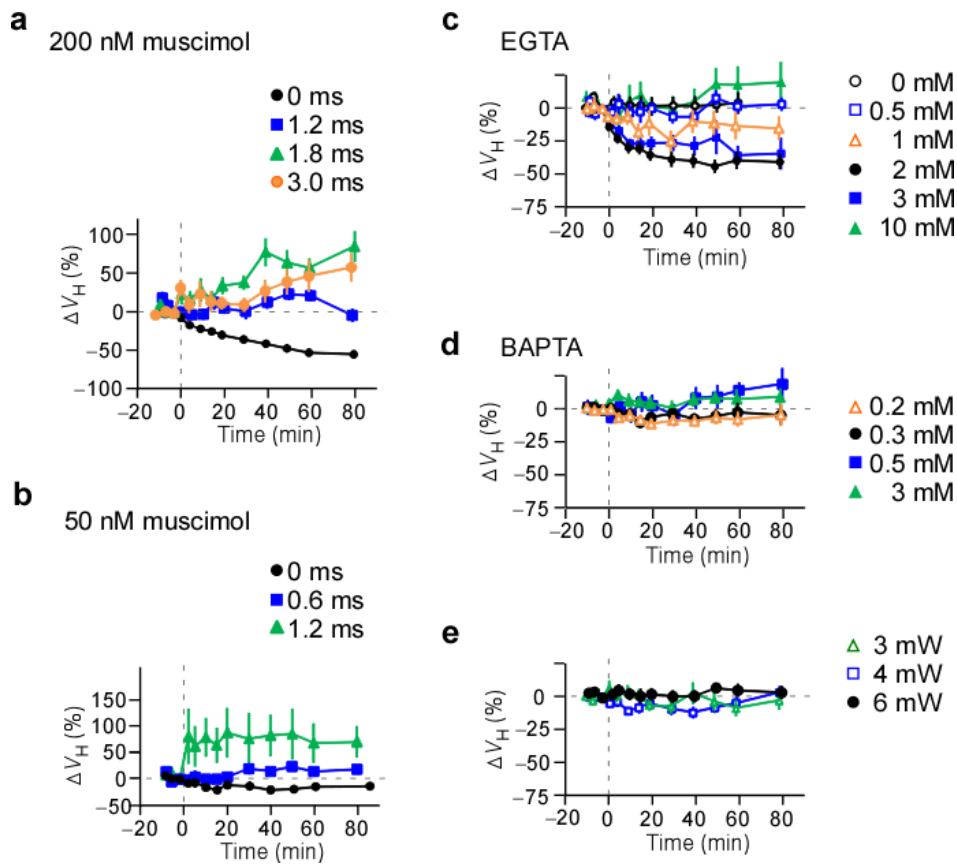
Supplementary Figure 6



Spine shrinkage in acute slice preparations

(a) Alexa 594 fluorescence images of a dendrite of acute slice preparation with one spine (magenta arrowhead) to which the LTD protocol was applied in the presence of muscimol (400 nM). The soma was located at the right side of the dendrite. (b) Time courses of spine shrinkage in the stimulated (s) and neighboring (n1-n8) spines shown in a. (c) The average time course of spine shrinkage in stimulated (7 spines, 7 dendrites, 7 slices, 7 rats) and neighboring spines (42 spines, 7 dendrites, 7 slices, 7 rats). Scale bar, 2 μm. (d) The average reductions in the spine volumes of stimulated ($n = 7$ spines) and neighboring spines at ≤ 3 μm ($n = 42$ spines), 3–10 μm ($n = 100$ spines), 10–15 μm ($n = 37$ spines), and ≥ 15 μm ($n = 17$ spines) from the stimulated spine. * $P < 0.05$, ** $P < 0.01$, *** $P < 0.001$ versus 0% by Wilcoxon signed-rank test.

Supplementary Figure 7

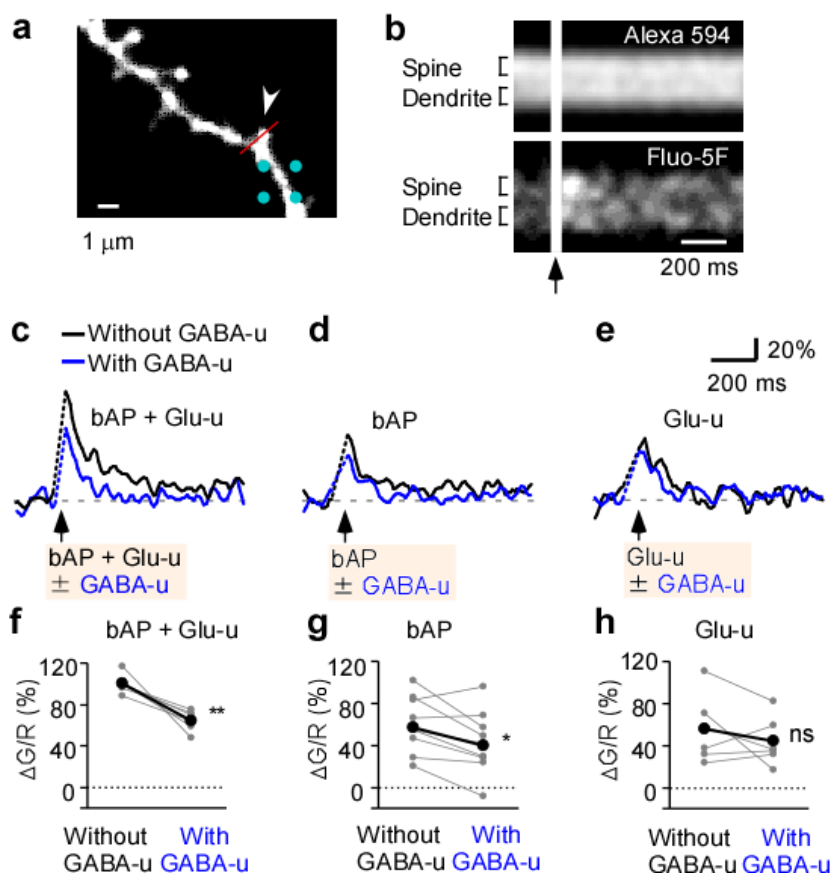


Spine shrinkage against enlargement or in the presence of Ca^{2+} buffers in the patch pipette

(a, b) Time courses of changes in volumes of the spines that were subjected to the LTP protocol and that were next to the one subjected to the LTD protocol in the presence of 200 nM in **a** or 50 nM muscimol in **b**. The durations of glutamate uncaging in the LTP protocol were 0 ms (38 spines, 16 dendrites, 16 slices, 13 rats), 1.2 ms (6 spines, 6 dendrites, 6 slices, 6 rats), 1.8 ms (8 spines, 8 dendrites, 8 slices, 7 rats), or 3 ms (6 spines, 6 dendrites, 6 slices, 6 rats) for 200 nM muscimol or 0 ms (17 spines, 7 dendrites, 7 slices, 4 rats), 0.6 ms (6 spines, 6 dendrites, 6 slices, 5 rats) or 1.2 ms (5 spines, 5 dendrites, 5 slices, 4 rats) in the presence of 50 nM muscimol. (c) Time courses of spine shrinkage in the presence of EGTA at 0 mM (15 spines, 10 dendrites, 5 slices, 3 rats), 0.5 mM (10 spines, 5 dendrites, 3 slices, 2 rats), 1 mM (11 spines, 4 dendrites, 2 slices, 2 rats), 2 mM (24 spines, 6 dendrites, 3 slices, 3 rats), 3 mM (21 spines, 7 dendrites, 4

slices, 3 rats), or 10 mM (9 spines, 4 dendrites, 1 slice, 1 rat) in the pipette. The external solution did not contain muscimol in **c–e**. **(d)** Time courses of spine shrinkage in the presence of BAPTA at 0.2 mM (38 spines, 12 dendrites, 4 slices, 4 rats), 0.3 mM (17 spines, 5 dendrites, 2 slices, 2 rats), 0.5 mM (23 spines, 7 dendrites, 2 slices, 2 rats), or 3 mM (18 spines, 6 dendrites, 2 slices, 2 rats) in the pipette. **(e)** Failure of induction of spine shrinkage by lowering the powers of glutamate uncaging in the LTD protocol to 6 mW (24 spines, 15 dendrites, 8 slices, 5 rats), 4 mW (28 spines, 6 dendrites, 2 slices, 2 rats), or 3 mW (15 spines, 6 dendrites, 2 slices, 2 rats).

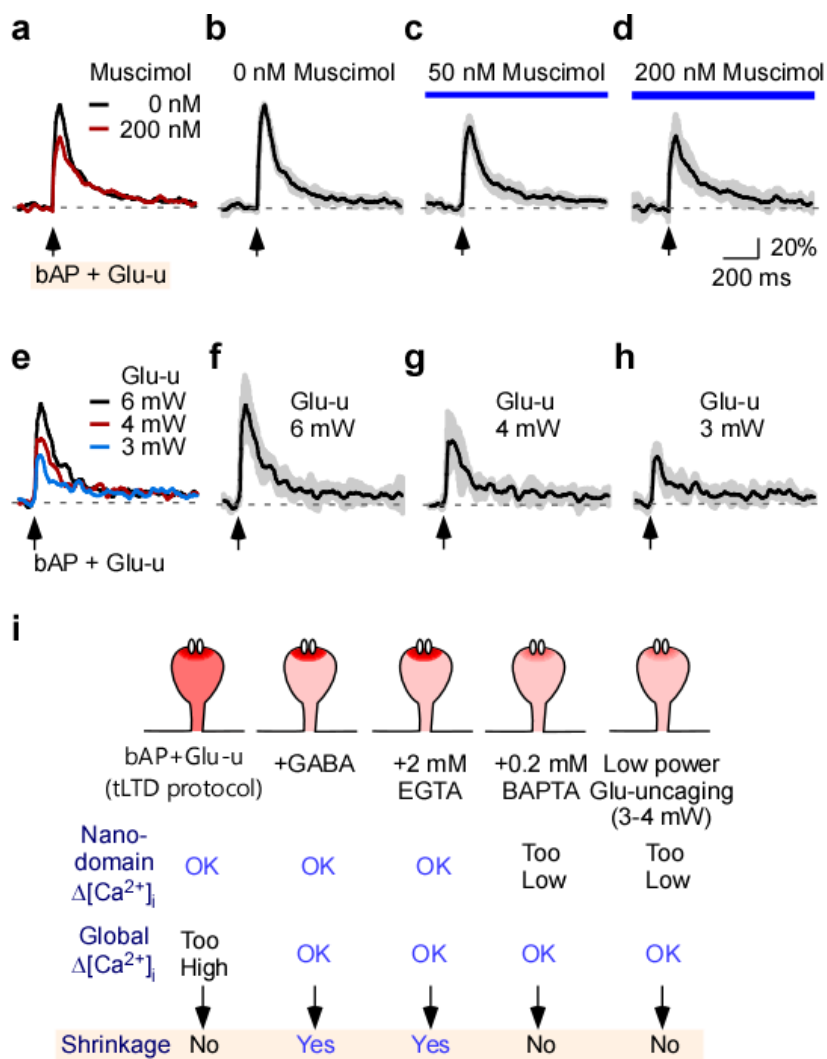
Supplementary Figure 8



Dependence of Ca^{2+} transients on GABA uncaging

(a) Alexa 594-fluorescent image of a dendrite to which a combination of bAPs and glutamate uncaging (Glu-u, arrow head) was applied with LTD timing and GABA uncaging (blue points) at bAP onset. (b) Line-scan imaging of Alexa 594 (20 μM , the upper image) and Fluo-5F (300 μM , the lower image) along the red line shown in a. (c–e) Time courses of fluorescent ratios between Fluo-5F and Alexa 594 without (black) or with (blue) GABA uncaging. The traces were averaged for bAP + Glu-u with the LTD timing in c (22 spines, 6 dendrites, 3 slices, 3 rats), bAP alone in d (25 spines, 9 dendrites, 5 slices, 5 rats), or Glu-u only in e (17 spines, 6 dendrites, 5 slices, 4 rats). The effects of GABA uncaging were examined in the same spines and averaged over a dendrite. The mean values of the ratios for bAP + Glu-u without GABA uncaging were normalized as 100% in d and e. The time period of GABA uncaging with a blue laser was connected with a dashed line. (f–h) Reduction in Ca^{2+} transients with GABA uncaging. * $P < 0.05$, ** $P < 0.01$ by paired t-test.

Supplementary Figure 9

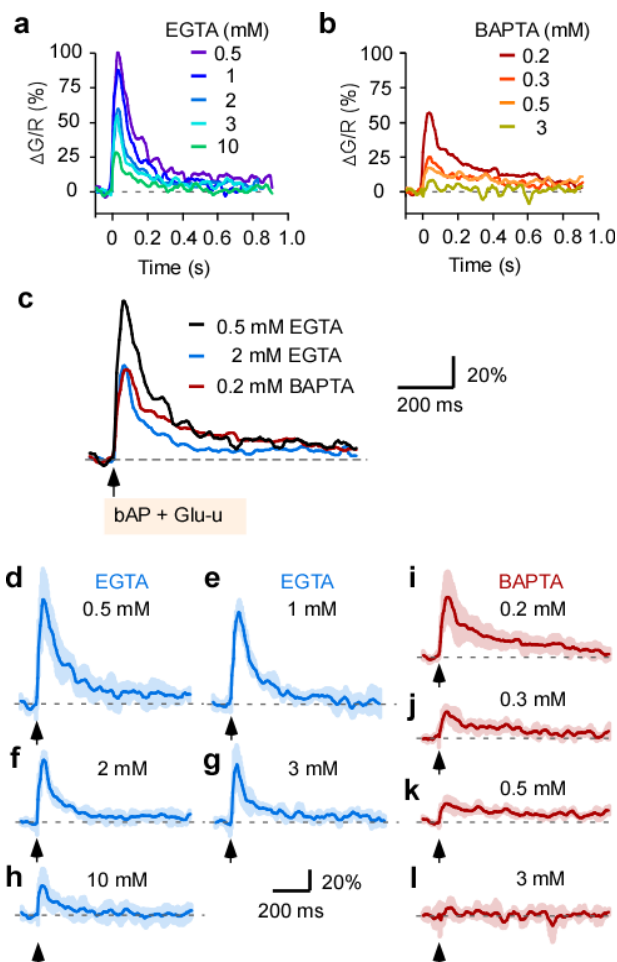


Effects of muscimol and laser powers on Ca^{2+} transients induced by pairing with LTD timing

(a) Time courses of fluo-5F/Alexa (G/R) ratios in dendritic spines in the presence of muscimol at 0 nM (black) or 200 nM (red) (18 spines, 7 dendrites, 7 slices, 2 rats). The traces were obtained both in the absence and presence of muscimol. The averaged traces over the dendrites are shown. The amplitudes are expressed relative to those in the absence of muscimol in the same dendrites (Fig. 6b). (b–d) Averaged time courses (thick lines) and standard deviations (shaded areas) of (G/R) ratios in the presence of muscimol at 0 nM in b, 50 nM in c (33 spines, 6 dendrites, 6 slices, 6 rats), and 200 nM

in **d**. **(e)** Time courses of fluo-5F/Alexa (G/R) ratios in dendritic spines induced with a combination of back-propagating action potentials (bAP) and Glu-u with the LTD timing with powers of 6, 4, and 3 mW from the same spines (30 spines, 5 dendrites, 5 slices, 3 rats). Each trace was averaged over all dendrites and normalized to the peak value for 6 mW uncaging (Fig. 7b). **(f–h)** Averaged time courses (thick lines) and standard deviations (shaded areas) of the (G/R) ratios in dendritic spines induced with a combination of bAP and Glu-u with the LTD timing with powers of 6 in **f**, 4 in **g**, and 3 mW in **h** from the same spines (30 spines, 5 dendrites, 5 slices, 3 rats). **(i)** Requirements of both nanodomain increases and global reduction in $[Ca^{2+}]_i$ in spine shrinkage. Ca^{2+} nanodomains act as sensors for glutamatergic synaptic input.

Supplementary Figure 10



Effects of Ca^{2+} buffers in the pipette on $[\text{Ca}^{2+}]_i$ increases in dendritic spines

The external solution did not contain muscimol for these experiments. (**a**, **b**) Time courses of fluo-5F/Alexa (G/R) ratios induced with a combination of bAPs and glutamate uncaging in the LTD protocol in the presence of EGTA with concentrations of 0.5 mM (32 spines, 5 dendrites, 3 slices, 3 rats), 1 mM (32 spines, 6 dendrites, 3 slices, 3 rats), 2 mM (37 spines, 6 dendrites, 3 slices, 3 rats), 3 mM (35 spines, 5 dendrites, 2 slices, 2 rats), or 10 mM (31 spines, 5 dendrites, 2 slices, 2 rats) in **a** or BAPTA with concentrations of 0.2 mM (63 spines, 8 dendrites, 4 slices, 4 rats), 0.3 mM (45 spines, 5 dendrites, 4 slices, 4 rats), 0.5 mM (39 spines, 5 dendrites, 3 slices, 3 rats), or 3 mM (28 spines, 5 dendrites, 2 slices, 2 rats) in **b** in the patch pipette. The mean ratios were

obtained first from each dendrite and averaged over all of the dendrites. The peak values were normalized to those for 0.5 mM EGTA. CaCl_2 was added to the buffer solutions to set the resting level of $[\text{Ca}^{2+}]_i$ to 30 nM (Methods). **(c)** Superimposed traces of (G/R) ratios induced with a combination of bAP and Glu-u in the LTD protocol in the absence (black) and presence of 2 mM EGTA (blue) and 0.2 mM BAPTA (red). **(d–l)** Averaged time courses (thick lines) and standard deviations (shaded areas) of (G/R) ratios.